Eur. Phys. J. C 56, 371–378 (2008)
DOI 10.1140/epjc/s10052-008-0654-y

THE EUROPEAN PHYSICAL JOURNAL C

Regular Article – Theoretical Physics

Associated production of prompt photons and heavy quarks in off-shell gluon–gluon fusion

This paper is dedicated to the memory of P.F. Ermolov, who died on May 14, 2008.

S.P. Baranov[1], A.V. Lipatov[2,a], N.P. Zotov[2]

[1] P.N. Lebedev Physics Institute, 119991 Moscow, Russia
[2] D.V. Skobeltsyn Institute of Nuclear Physics, M.V. Lomonosov Moscow State University, Leninskie gory, 119991 Moscow, Russia

Received: 17 May 2008 /
Published online: 17 July 2008 –

Abstract. In the framework of the k_{T}-factorization approach, we study the production of prompt photons associated with heavy (charm and beauty) quarks in hadron–hadron collisions at high energies. Our consideration is based on the amplitude for the production of a single photon associated with a quark pair in the fusion of two off-shell gluons. The total and differential cross sections are presented and the conservative error analysis is performed. Two sets of unintegrated gluon distributions in the proton have been used in numerical calculation: the one obtained from Ciafaloni–Catani–Fiorani–Marchesini evolution equation and the other from Kimber–Martin–Ryskin prescription. The theoretical results are compared with recent experimental data taken by the CDF collaboration at the Fermilab Tevatron. Our analysis extends to specific angular correlations between the produced prompt photons and muons originating from semileptonic decays of the final charmed or beauty quarks. We point out the importance of such observables, which can serve as a crucial test for the unintegrated gluon densities in a proton. Finally, we extrapolate the theoretical predictions to the CERN LHC energies.

PACS. 12.38.Bx; 13.85.Qk

1 Introduction

The production of prompt (or direct) photons in hadron–hadron collisions at the Tevatron is a subject of intense studies on both the theoretical and experimental sides [1–10]. Usually the photons are called "prompt" if they are coupled to the interacting quarks. The theoretical and experimental investigations of such processes have provided a direct probe of the hard subprocess dynamics, since the produced photons are largely insensitive to the effects of final-state hadronization. At the leading order of perturbative quantum chromodynamics (pQCD), prompt photons can be produced via quark–gluon Compton scattering or quark–antiquark annihilation and so, the cross sections of these processes are strongly sensitive to the parton (quark and gluon) content of a proton.[1] The perturbative QCD calculations [12–15] in the next-to-leading order (NLO) approximation agree with the recent high-p_{T} measurements [6] within uncertainties (see also discussions in [16–20]). However, there are still open questions. It was found [1–4] that the shape of the measured cross section as a function of photon transverse energy E_{T} is poorly described by the NLO pQCD calculations: the observed E_{T} distribution is steeper than the predictions. This shape difference leads to a significant disagreement in the ratio of the cross sections calculated at different center-of-mass energies $\sqrt{s} = 630\,\mathrm{GeV}$ and $\sqrt{s} = 1800\,\mathrm{GeV}$ as a function of scaling variable $x_{\mathrm{T}} = 2E_{\mathrm{T}}^{\gamma}/\sqrt{s}$. It was demonstrated [2,3] that the disagreement in the x_{T} ratio is difficult to explain with the conventional theoretical uncertainties coming from the scale dependence and different parametrizations of the parton distributions. In the NLO QCD approximation, the observed discrepancy can be reduced [17,21] by attributting some additional intrinsic transverse momentum k_{T} to the incoming partons, which is usually assumed to have a Gaussian-like distribution. The average value of this k_{T} increases from $\langle k_{\mathrm{T}} \rangle \sim 1\,\mathrm{GeV}$ to more than $\langle k_{\mathrm{T}} \rangle \sim 3\,\mathrm{GeV}$ [17,20] as the $\sqrt{s}$ increases from UA6 to Tevatron energies.[2]

[a] email: lipatov@theory.sinp.msu.ru

[1] Also, the observed photon may arise from the so called fragmentation processes [11]. This contribution will be discussed below in Sect. 2.

[2] The importance of including the gluon emission through the resummation formalism was recognized and only recently this approach has been developed [21–25] for inclusive prompt photon production.

From our point of view, a more adequate solution was found [26–29] in the framework of the $k_{\rm T}$-factorization approach [30–33]. This approach is based on the familiar Balitsky–Fadin–Kuraev–Lipatov (BFKL) [34–36] or Ciafaloni–Catani–Fiorani–Marchesini (CCFM) [37–40] gluon evolution equations and takes into account the large logarithmic terms proportional to $\ln 1/x$. It is believed that such terms give a significant contribution to the heavy quark production cross section at the conditions of modern colliders. This contrasts with the usual Dokshitzer–Gribov–Lipatov–Altarelli–Parizi (DGLAP) [41–44] strategy where only the large logarithmic terms proportional to $\ln \mu^2$ are taken into account. The basic dynamical quantity of the $k_{\rm T}$-factorization approach is the unintegrated (i.e., $\mathbf{k}_{\rm T}$-dependent) gluon distribution $\mathcal{A}(x, \mathbf{k}_{\rm T}^2, \mu^2)$ which determines the probability to find a gluon carrying the longitudinal momentum fraction x and the transverse momentum $\mathbf{k}_{\rm T}$ at the probing scale μ^2. Similar to DGLAP, to calculate the cross sections of any physical process the unintegrated gluon density $\mathcal{A}(x, \mathbf{k}_{\rm T}^2, \mu^2)$ has to be convoluted [30–33] with the relevant partonic cross section which has to be taken off mass shell ($\mathbf{k}_{\rm T}$-dependent). Since the gluons in the initial state are not on-shell and are characterized by virtual masses (proportional to their transverse momentum), it also assumes a modification of their polarization density matrix [30–33]. In particular, the polarization vector of a gluon is no longer purely transversal, but acquires an admixture of longitudinal and time-like components. Other important properties of the $k_{\rm T}$-factorization formalism are the additional contribution to the cross sections due to the integration over the $\mathbf{k}_{\rm T}^2$ region above μ^2 and the broadening of the transverse momentum distributions due to extra transverse momentum of the colliding partons.

In this approach, the treatment of the $k_{\rm T}$-enhancement suggests a modification of the simple $k_{\rm T}$ smearing picture described above: the transverse momentum $k_{\rm T}$ of the incoming partons is generated in the course of non-collinear parton evolution under control of the corresponding evolution equation. First calculations of the inclusive prompt photon production at the Tevatron within the $k_{\rm T}$-factorization formalism have been performed in [26–29]. The calculations [26–28] were based on the $q + g^* \to \gamma + q$ and $q + \bar{q} \to \gamma + g$ off-shell matrix elements.[3] A reasonable agreement was found [28] between the theoretical predictions and the available D$\varnothing$ and CDF experimental data [1–6] in both the central and forward pseudorapidity η^γ regions. Perfect agreement was found also in the ratio of the cross sections calculated at $\sqrt{s} = 630\,\text{GeV}$ and $\sqrt{s} = 1800\,\text{GeV}$. However, an important component of the calculations [26–28] is the unintegrated quark distribution in a proton which at present is available in the framework of Kimber–Martin–Ryskin (KMR) [45, 46] approach only.[4] In contrast with [26–28], the central part of our previous consideration [29] is the off-shell gluon–gluon fusion subprocess $g^* + g^* \to \gamma + q\bar{q}$. At the price of considering the $2 \to 3$ rather than $2 \to 2$ matrix elements, the problem of unknown unintegrated quark distributions has been reduced to the problem of gluon distributions. In this way, since the gluons are only responsible for the appearance of the sea but not valence quarks, the contribution from the valence quarks should be calculated separately. Having in mind that the valence quarks are only important at large x, where the traditional DGLAP evolution is accurate and reliable, this contribution has been calculated within the usual collinear scheme based on $2 \to 2$ partonic subprocesses and on-shell parton densities. Thus, the way proposed in [29] enables us with making comparisons between the different parton evolution schemes and parametrizations of parton densities, in contrast with previous calculations [26, 28] where such a comparison was not possible. It is important that the predictions [29] based on the off-shell gluon–gluon fusion matrix element $g^* + g^* \to \gamma + q\bar{q}$ and the KMR gluon density agree with the previous results [28] based on the $2 \to 2$ subprocesses. This can be regarded as an additional proof of the consistency of the proposed method.

In the present paper we will apply the formalism [29] described above to investigate the prompt photon and associated heavy (charm and beauty) quark production at high energies. The experimental data on the $\gamma + c$ and $\gamma + b$ cross sections as a function of photon transverse momentum $p_{\rm T}$ have been reported recently [9, 10] by the CDF collaboration. Also, there are available data [7, 8] on the associated prompt photon and muon production at the Tevatron, where the final state muon originates from the semileptonic decay of a charmed or beauty quark. Both these measurements are sensitive to the physics beyound the standard model (SM), for example the production of excited quarks or gauge-mediated supersymmetry breaking (GMSB) with neutralinos radiatively decaying to gravitinos [48]. Therefore, it is necessary to have a realistic estimation of the associated $\gamma + Q$ or $\gamma + \mu$ production cross sections within QCD. An additional motivation for our investigations is the fact that these processes provide a direct probe of the off-shell matrix elements $g^* + g^* \to \gamma + q\bar{q}$ since there is no contribution from valence quarks. In order to investigate the underlying dynamics in more detail, we study the angular correlations between the transverse momenta of the prompt photon and the final muon. These quantities are sensitive to the production mechanism and, also, powerful tests for the non-collinear evolution [49].

The outline of our paper is following. In Sect. 2 we recall shortly the basic formulas of the $k_{\rm T}$-factorization approach with a brief review of calculation steps. In Sect. 3 we present the numerical results of our calculations and a discussion. Section 4 contains our conclusions.

2 Theoretical framework

2.1 Kinematics

First, we recall in brief some technical details of our previous paper [29] needed below. We start from the kinematics

[3] In the calculations [26], the usual on-shell matrix elements were embedded in precise off-shell kinematics.

[4] Unintegrated quark density was also considered recently in [47].

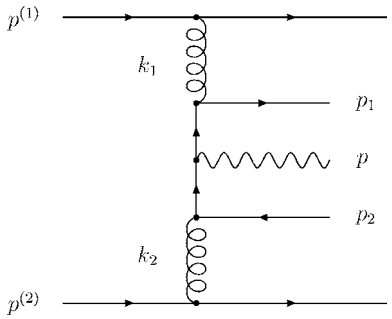

Fig. 1. Kinematics of the $g^* + g^* \to \gamma + Q\bar{Q}$ process

(see Fig. 1). Let $p^{(1)}$ and $p^{(2)}$ be the four-momenta of the incoming protons and p the four-momentum of the produced photon. The initial off-shell gluons have the four-momenta k_1 and k_2 and the final quark Q and antiquark $\bar{Q}$ have the four-momenta p_1 and p_2 and the mass m_Q, respectively. In the $p\bar{p}$ center-of-mass frame we can write

$$p^{(1)} = \frac{\sqrt{s}}{2}(1,0,0,1)\,, \quad p^{(2)} = \frac{\sqrt{s}}{2}(1,0,0,-1)\,, \qquad (1)$$

where $\sqrt{s}$ is the total energy of the process under consideration and we neglect the masses of the incoming protons. The initial gluon four-momenta in the high energy limit can be written as

$$k_1 = x_1 p^{(1)} + k_{1\mathrm{T}}\,, \quad k_2 = x_2 p^{(2)} + k_{2\mathrm{T}}\,, \qquad (2)$$

where $k_{1\mathrm{T}}$ and $k_{2\mathrm{T}}$ are the transverse four-momenta. It is important that $\mathbf{k}_{1\mathrm{T}}^2 = -k_{1\mathrm{T}}^2 \neq 0$ and $\mathbf{k}_{2\mathrm{T}}^2 = -k_{2\mathrm{T}}^2 \neq 0$. From the conservation laws we obtain the following relations:

$$\begin{aligned} \mathbf{k}_{1\mathrm{T}} + \mathbf{k}_{2\mathrm{T}} &= \mathbf{p}_{1\mathrm{T}} + \mathbf{p}_{2\mathrm{T}} + \mathbf{p}_{\mathrm{T}}\,, \\ x_1\sqrt{s} &= m_{1\mathrm{T}}\mathrm{e}^{y_1} + m_{2\mathrm{T}}\mathrm{e}^{y_2} + |\mathbf{p}_{\mathrm{T}}|\mathrm{e}^{y}\,, \\ x_2\sqrt{s} &= m_{1\mathrm{T}}\mathrm{e}^{-y_1} + m_{2\mathrm{T}}\mathrm{e}^{-y_2} + |\mathbf{p}_{\mathrm{T}}|\mathrm{e}^{-y}\,, \end{aligned} \qquad (3)$$

where y is the rapidity of produced photon, $p_{1\mathrm{T}}$ and $p_{2\mathrm{T}}$ are the transverse four-momenta of final quark and antiquark, y_1, y_2, $m_{1\mathrm{T}}$ and $m_{2\mathrm{T}}$ are their center-of-mass rapidities and transverse masses, i.e. $m_{i\mathrm{T}}^2 = m_Q^2 + \mathbf{p}_{i\mathrm{T}}^2$.

2.2 Cross section for associated $\gamma + Q$ production

In general, according to the k_{T}-factorization theorem, the photon-quark associated production cross section can be written as a convolution

$$\begin{aligned} &\sigma(p + \bar{p} \to \gamma + Q + X) \\ &= \int \frac{\mathrm{d}x_1}{x_1} \mathcal{A}\left(x_1, \mathbf{k}_{1\mathrm{T}}^2, \mu^2\right) \mathrm{d}\mathbf{k}_{1\mathrm{T}}^2 \frac{\mathrm{d}\phi_1}{2\pi} \\ &\quad \times \int \frac{\mathrm{d}x_2}{x_2} \mathcal{A}\left(x_2, \mathbf{k}_{2T}^2, \mu^2\right) \\ &\quad \times \mathrm{d}\mathbf{k}_{2T}^2 \frac{\mathrm{d}\phi_2}{2\pi} \mathrm{d}\hat{\sigma}(g^* + g^* \to \gamma + Q\bar{Q})\,, \end{aligned} \qquad (4)$$

where $\hat{\sigma}(g^* + g^* \to \gamma + Q\bar{Q})$ is the partonic cross section, $\mathcal{A}\big(x, \mathbf{k}_{\mathrm{T}}^2, \mu^2\big)$ is the unintegrated gluon distribution in a proton and ϕ_1 and ϕ_2 are the azimuthal angles of the incoming gluons. The multiparticle phase space $\Pi\, \mathrm{d}^3 p_i / 2E_i \delta^{(4)}(\sum p^{\mathrm{in}} - \sum p^{\mathrm{out}})$ is parametrized in terms of transverse momenta, rapidities and azimuthal angles:

$$\frac{\mathrm{d}^3 p_i}{2E_i} = \frac{\pi}{2} \mathrm{d}\mathbf{p}_{i\mathrm{T}}^2 \mathrm{d}y_i \frac{\mathrm{d}\phi_i}{2\pi}\,. \qquad (5)$$

Using the expressions (4) and (5) we obtain the master formula:

$$\begin{aligned} &\sigma(p + \bar{p} \to \gamma + Q) \\ &= \int \frac{1}{256\pi^3 (x_1 x_2 s)^2} |\bar{\mathcal{M}}(g^* + g^* \to \gamma + Q + \bar{Q})|^2 \\ &\quad \times \mathcal{A}\left(x_1, \mathbf{k}_{1\mathrm{T}}^2, \mu^2\right) \mathcal{A}\left(x_2, \mathbf{k}_{2\mathrm{T}}^2, \mu^2\right) \mathrm{d}\mathbf{k}_{1\mathrm{T}}^2 \mathrm{d}\mathbf{k}_{2\mathrm{T}}^2 \mathrm{d}\mathbf{p}_{1\mathrm{T}}^2 \mathbf{p}_{2\mathrm{T}}^2 \\ &\quad \times \mathrm{d}y \mathrm{d}y_1 \mathrm{d}y_2 \frac{\mathrm{d}\phi_1}{2\pi} \frac{\mathrm{d}\phi_2}{2\pi} \frac{\mathrm{d}\psi_1}{2\pi} \frac{\mathrm{d}\psi_2}{2\pi}\,, \end{aligned} \qquad (6)$$

where $|\bar{\mathcal{M}}(g^* + g^* \to \gamma + Q + \bar{Q})|^2$ is the off-mass shell matrix element squared and averaged over the initial gluon polarizations and colors, ψ_1 and ψ_2 are the azimuthal angles of the final state quark and antiquark, respectively.

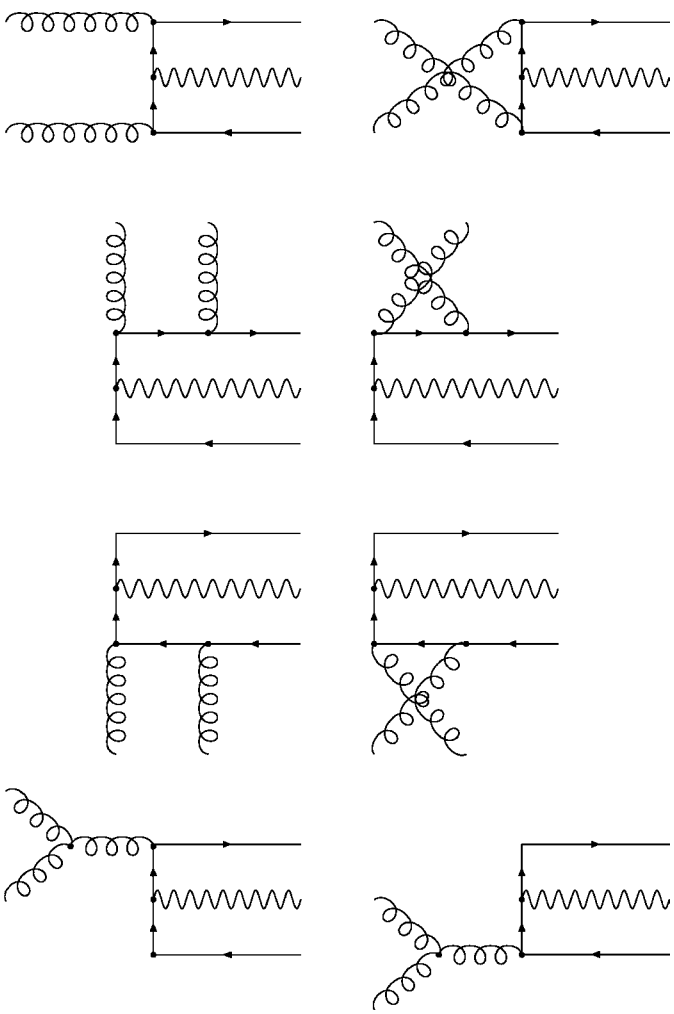

Fig. 2. Feynman diagrams which describe the partonic subprocess $g^* + g^* \to \gamma + Q\bar{Q}$ at the leading order in α_{s} and α

Concerning the amplitude $g^* + g^* \to \gamma + Q\bar{Q}$, there are eight Feynman diagrams which describe this partonic subprocess at the leading order in α_s and α (see Fig. 2). The analytic expression for the $|\bar{\mathcal{M}}(g^* + g^* \to \gamma + Q + \bar{Q})|^2$ has been derived in our previous paper [29]. We only mention here that, in accord with the k_T-factorization prescription [30–33], the off-shell gluon spin density matrix has been taken in the form

$$\sum \epsilon^\mu(k_i)\epsilon^{*\,\nu}(k_i) = \frac{k_{iT}^\mu k_{iT}^\nu}{\mathbf{k}_{iT}^2}\,. \tag{7}$$

In all other respects our calculations follow the standard Feynman rules. If we average the expression (6) over ϕ_1 and ϕ_2 and take the limit $\mathbf{k}_{1T}^2 \to 0$ and $\mathbf{k}_{2T}^2 \to 0$, then we recover the relevant expression in the usual collinear approximation.

The multidimensional integration in (6) has been performed by the means of Monte Carlo technique, using the routine VEGAS [50]. The full C++ code is available from the authors on request.[5] This code is practically identical to that used in [29], with exception that now we apply it to calculate the cross section of prompt photon and heavy quark (or rather decay muon) associated production.

2.3 Photon isolation and fragmentation contribution

In order to reduce huge background from the secondary photons produced by the decays of π^0 and η mesons, the isolation criterion is introduced in the experimental analyses. This criterion is the following. A photon is isolated if the amount of hadronic transverse energy E_T^{had} deposited inside a cone with aperture R centered around the photon direction in the pseudo-rapidity and azimuthal angle plane is smaller than some value E_T^{max}:

$$\begin{aligned} &E_T^{had} \le E_T^{max}\,,\\ &(\eta^{had} - \eta)^2 + (\phi^{had} - \phi)^2 \le R^2\,. \end{aligned} \tag{8}$$

The CDF collaboration takes $R = 0.4$ and $E_T^{max} = 1\,\text{GeV}$ in the experiment [8–10] and $R = 0.7$ and $E_T^{max} = 2\,\text{GeV}$ in the earlier experiment [7].

It is important that there is an additional mechanism of photon production not described above. It is the fragmentation of a partonic jet into a single photon carrying a large fraction z of the jet energy [8]. These processes are described in terms of quark-to-photon $D_{q\to\gamma}(z,\mu^2)$ and gluon-to-photon $D_{g\to\gamma}(z,\mu^2)$ fragmentation functions. However, the isolation condition(8) not only reduces the background but also significantly reduces the fragmentation components. It was shown [51] that after applying the isolation cut the contribution from the fragmentation subprocesses is strongly suppressed (this contribution amounts to about 10% of the visible cross section). Therefore in further analysis we will not consider the fragmentation component.

[5] lipatov@theory.sinp.msu.ru

3 Numerical results

3.1 Theoretical uncertainties

There are several parameters which determine the overall normalization factor of the cross section (6): the unintegrated gluon distribution in a proton $\mathcal{A}(x,\mathbf{k}_T^2,\mu^2)$, the factorization and renormalization scales μ_F and μ_R and the heavy quark mass m_Q.

Concerning the unintegrated gluon densities in a proton, we have tried here two different sets of them. These sets are widely discussed in the literature (see, for example, review [52–54] for more information). Here we only shortly discuss their characteristic properties.

One set has been obtained [55] recently from the numerical solution of the CCFM equation. Function $\mathcal{A}(x,\mathbf{k}_T^2,\mu^2)$ is determined by a convolution of the non-perturbative starting distribution $\mathcal{A}_0(x)$ and the CCFM evolution kernel denoted by $\tilde{\mathcal{A}}(x,\mathbf{k}_T^2,\mu^2)$:

$$\mathcal{A}\left(x,\mathbf{k}_T^2,\mu^2\right) = \int \frac{\mathrm{d}x'}{x'}\mathcal{A}_0(x')\tilde{\mathcal{A}}\left(\frac{x}{x'},\mathbf{k}_T^2,\mu^2\right). \tag{9}$$

In the perturbative evolution the gluon splitting function $P_{gg}(z)$ including non-singular terms (as it was described in [56]) is applied. The input parameters in $\mathcal{A}_0(x)$ were fitted to reproduce the proton structure functions $F_2(x,Q^2)$. An acceptable fit to the measured F_2 values was obtained [55] with $\chi^2/\text{ndf} = 1.83$ using statistical and uncorrelated systematic uncertainties (compare to $\chi^2/\text{ndf} \sim 1.5$ in the collinear approach at NLO).

Another set (the so-called KMR distribution) is the one which was originally proposed in [45, 46]. The KMR approach is a formalism to construct unintegrated gluon distribution from the known conventional parton (quark and gluon) densities. It accounts for the angular-ordering (which comes from the coherence effects in gluon emission) as well as the main part of the collinear higher-order QCD corrections. The key observation here is that the μ dependence of the unintegrated parton distribution enters at the last step of the evolution and therefore single scale evolution equations can be used up to this step.[6]

Significant theoretical uncertainties are connected with the choice of the factorization and renormalization scales. The first of them is related to the evolution of the gluon distributions, the other is responsible for the strong coupling constant $\alpha_s(\mu_R^2)$. As it is often done, we choose the renormalization and factorization scales to be equal: $\mu_R = \mu_F = \mu = \xi|\mathbf{p}_T|$. In order to investigate the scale dependence of our results we will vary the scale parameter ξ between 1/2 and 2 about the default value $\xi = 1$.

In the numerical calculations we set the charm and beauty quark masses to $m_c = 1.4\,\text{GeV}$ and $m_b = 4.75\,\text{GeV}$. We have checked that the uncertainties which come from these quantities are negligible in comparison with the uncertainties connected with the unintegrated gluon distributions. For completeness, we use the LO formula for the

[6] In the numerical calculations we have used the standard GRV (LO) parametrizations [57, 58] of the collinear quark and gluon densities.

strong coupling constant $\alpha_s(\mu^2)$ with $n_f = 4$ active quark flavors at $\Lambda_{QCD} = 200\,\text{MeV}$ (so that $\alpha_s(M_Z^2) = 0.1232$). Note that we use the special choice $\Lambda_{QCD} = 130\,\text{MeV}$ in the case of CCFM gluon ($\alpha_s(M_Z^2) = 0.1187$), as it was originally proposed in [55].

3.2 Associated $\gamma + Q$ production at Tevatron

We are now in a position to present our numerical results. Figures 3 and 4 confront the $\gamma + c$ and $\gamma + b$ production cross sections calculated as a function of the photon transverse energy E_T with the preliminary experimental data [9, 10] taken by the CDF collaboration at the Tevatron Run II ($\sqrt{s} = 1960\,\text{GeV}$). These data refer to the central kinematic region defined by $|\eta^\gamma| < 1$. The solid and dotted histograms correspond to the results obtained with the CCFM and KMR unintegrated gluon densities, respectively. The upper and lower dashed histograms correspond to the scale variations in CCFM density as it was described above. We find that the CCFM-evolved unintegrated gluon density reproduces well the data within the theoretical and experimental uncertainties, and that the KMR density tends to underestimate the data in wide E_T range. A similar effect was observed also in the case of inclusive prompt photon production [29]. The difference between the CCFM and KMR predictions is directly connected with the small-x behaviour of these gluon densities and demonstrates the importance of leading $\ln 1/x$ terms. Of course, the scale uncertainties of our predictions are significant. The latter can be reduced by considering the ratio of the cross sections $\gamma + c$ to $\gamma + b$. This ratio is a subject of special interest: one could expect from the ratio of the quark charges that the $\gamma + c$ events should be 4 times more often than the $\gamma + b$ events. In addition to that, there must be extra suppression of the $\gamma + b$ events due to heavier b mass (in the $g + g \to \gamma + Q\bar{Q}$ approach) or smaller beauty content in the proton sea (in the $g + Q \to \gamma + Q$ approach). Our prediction for the ratio $\sigma(\gamma + c)/\sigma(\gamma + b)$ is shown in Fig. 5 in comparison with the CDF data [9, 10]. Both the CCFM and KMR gluon densities predict this ratio to be equal to 6 : 1 or 7 : 1 in a wide E_T range. This result is consistent with the measurement [9, 10].

There are also available CDF data [7, 8] on the muons which originate from the semileptonic decays of charmed or beauty quarks. The experimental data [8] refer to the kinematic region $p_T^\mu > 4\,\text{GeV}$, $|\eta^\gamma| < 0.9$, $|\eta^\mu| < 1.0$ and $\sqrt{s} = 1800\,\text{GeV}$. In Fig. 6 we show the $\gamma + \mu$ cross section as a function of photon transverse momentum p_T. The contributions from both the $\gamma + c$ and $\gamma + b$ events have been taken into account. To produce muons from charmed and beauty quarks in our theoretical calculations, we first

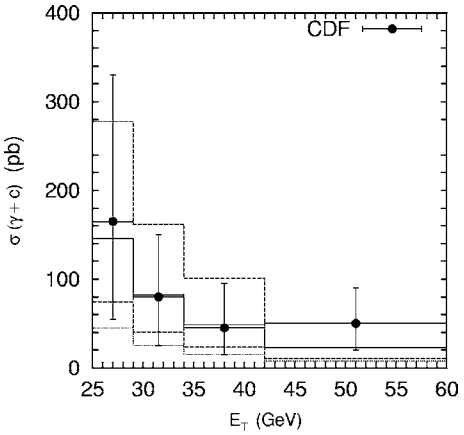

Fig. 3. The $\sigma(\gamma + c)$ cross section as a function of the photon transverse energy E_T at $|\eta| < 1.0$ and $\sqrt{s} = 1960\,\text{GeV}$. The *solid* and *dotted histograms* correspond to the CCFM and KMR gluon densities, respectively, with the default scale $\mu = E_T$. The *upper* and *lower dashed histograms* correspond to the scale variation in the CCFM distribution. The experimental data are from CDF [9, 10]

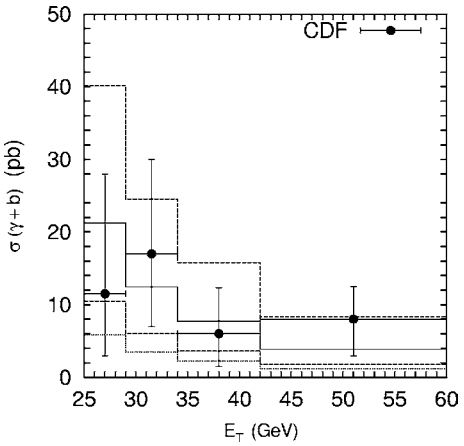

Fig. 4. The $\sigma(\gamma + b)$ cross section as a function of the photon transverse energy E_T at $|\eta| < 1.0$ and $\sqrt{s} = 1960\,\text{GeV}$. The notation of the histograms is the same as in Fig. 3. The experimental data are from CDF [9, 10]

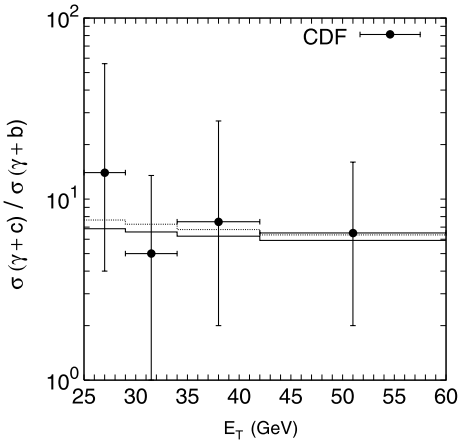

Fig. 5. The ratio of $\gamma + c$ to $\gamma + b$ cross sections as a function of the photon transverse energy E_T at $|\eta| < 1.0$ and $\sqrt{s} = 1960\,\text{GeV}$. The *solid* and *dotted histograms* correspond to the CCFM and KMR gluon densities, respectively, with the default scale $\mu = E_T$. The experimental data are from CDF [9, 10]

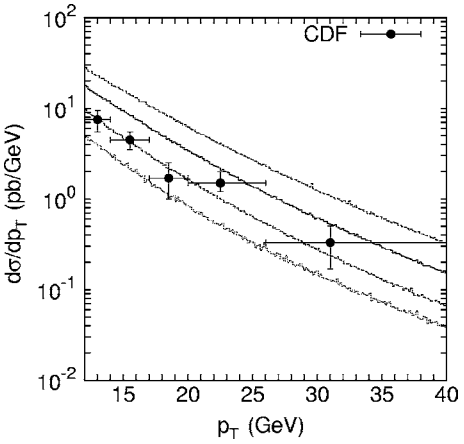

Fig. 6. The differential cross section $\mathrm{d}\sigma/\mathrm{d}p_{\mathrm{T}}$ for associated prompt photon and muon hadroproduction calculated at $p_{\mathrm{T}}^{\mu} > 4\,\mathrm{GeV}$, $|\eta^{\gamma}| < 0.9$, $|\eta^{\mu}| < 1.0$ and $\sqrt{s} = 1800\,\mathrm{GeV}$. The notation of the histograms is the same as in Fig. 3. The experimental data are from CDF [8]

convert them into a D or B hadrons using the Peterson fragmentation function [59] and then simulate their semileptonic decay according to the standard electroweak theory.[7] As usual, we set the fragmentation parameter ϵ to $\epsilon_c = 0.06$ and $\epsilon_b = 0.006$. The branching fractions $f(c \to \mu)$ and $f(b \to \mu)$ were set to $f(c \to \mu) = 0.09$ and $f(b \to \mu) = 0.1078$ [60]. One can see that in the case of $\gamma + \mu$ production, our predictions with the CCFM gluon density slightly overestimate the data but still agree with them within the uncertainties. The collinear NLO QCD calculations [61] give similar description of the data. The results obtained with the KMR density lie below the measurements and are similar to those [8] obtained from the PYTHIA Monte Carlo [62].

An important point of our consideration is the investigation of the angular correlations between the prompt photon and heavy quark. It is well known that studying these correlations gives additional insight into the production dynamics and, in particular, into the effective contributions from higher-order QCD processes. For example, the lowest-order QCD production diagrams $g + Q \to \gamma + Q$ contain only the photon γ and heavy quark Q in the final state. Therefore, the distribution over $\Delta\phi = \phi_{\gamma} - \phi_Q$ must be simply a delta function $\delta(\Delta\phi - \pi)$ since the produced particles are back-to-back in the transverse plane and are balanced in p_{T} due to momentum conservation. When higher-order QCD processes are considered, the presence of additional quarks and/or gluons in the final state allows the $\Delta\phi$ distribution to be more spread and the heavy quark transverse momenta more asymmetric. In the k_{T}-factorization formalism, taking into account the non-vanishing initial gluon transverse momentum $\mathbf{k}_{\mathrm{T}}$ leads to the violation of back-to-back kinematics even at leading order. However, using the $2 \to 3$ matrix elements instead the $2 \to 2$ ones (as it was described above) makes the difference between the k_{T}-factorization predictions and the collinear approximation of QCD (in $\alpha_{\mathrm{em}}\alpha_s^2$ approximation) not well pronounced.

The associated $\gamma + \mu$ cross section as a function of the azimuthal angle $\Delta\phi(\gamma - \mu)$ has been measured in [7]. The data on the normalized differential cross section $(1/\sigma)\,\mathrm{d}\sigma/\mathrm{d}\Delta\phi(\gamma - \mu)$ have been presented. These data refer to the kinematic region $17 < E_{\mathrm{T}} < 40\,\mathrm{GeV}$, $p_{\mathrm{T}}^{\mu} > 4\,\mathrm{GeV}$, $|\eta^{\gamma}| < 0.9$, $|\eta^{\mu}| < 1.0$ and $\sqrt{s} = 1800\,\mathrm{GeV}$. Our theoretical prediction compared to the data are shown in Fig. 7. We find here a number of the interesting points. First, the shapes of histograms predicted by the CCFM and KMR gluon densities are very different from each other. The CCFM gluon reproduces well the shape of the measured $\Delta\phi$ distribution, although tends to slightly overestimate the data at $\Delta\phi \sim \pi$, while the KMR gluon density is unable to describe the data anywhere. The observed shape difference is in contrast with the transverse momentum spectra, where both the unintegrated gluon distributions under consideration demonstrate a (more or less) similar behaviour. This fact clearly indicates that the $\gamma + \mu$ cross section as a function of $\Delta\phi$ is very sensitive to the details of the non-collinear evolution. A similar observation has been made earlier [49] in the case of b-quark hadroproduction at the Tevatron. Thus, futher theoretical and experimental studying such quantities can give us the possibility to additional constrain the unintegrated gluon densities. However, we should mention that the behaviour of the $\Delta\phi$ distribution at $\Delta\phi \sim 0$ depends sensibly on the photon isolation criteria. In particular, it depends on the parameters R and $E_{\mathrm{T}}^{\mathrm{max}}$ determining the cone isolation (8). Our predictions for LHC energy are shown in Figs. 8 and 9.

In conclusion, we would like to stress a number of important achievements shown by the k_{T}-factorization approach. As a general feature, the model behaviour is found

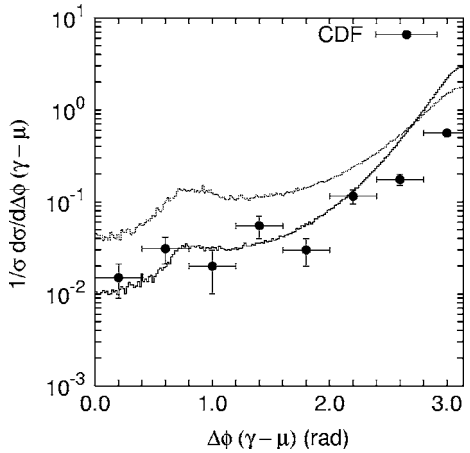

Fig. 7. The difference in azimuthal angle $\Delta\phi(\gamma - \mu)$ between the photon and muon calculated at $17\,\mathrm{GeV} < p_{\mathrm{T}} < 40\,\mathrm{GeV}$, $p_{\mathrm{T}}^{\mu} > 4\,\mathrm{GeV}$, $|\eta^{\gamma}| < 0.9$, $|\eta^{\mu}| < 1.0$ and $\sqrt{s} = 1800\,\mathrm{GeV}$. The notation of the histograms is the same as in Fig. 5. The experimental data are from CDF [7]

[7] Of course, the muon transverse momentum spectra are sensitive to the fragmentation functions. However, this dependence is expected to be small as compared with the uncertainties coming from the unintegrated gluon densities in a proton.

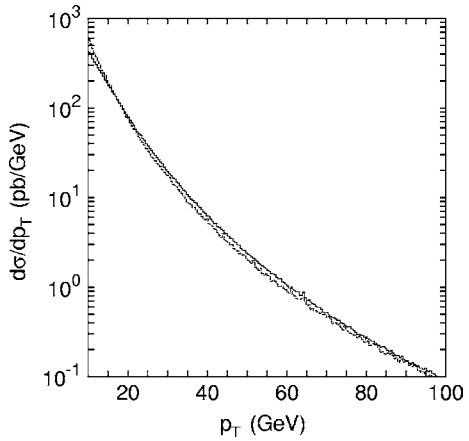

Fig. 8. The differential cross section $\mathrm{d}\sigma/\mathrm{d}p_{\mathrm{T}}$ for associated prompt photon and muon hadroproduction calculated at $p_{\mathrm{T}}^{\mu} > 4\,\mathrm{GeV}$, $|\eta^{\gamma}| < 2.5$, $|\eta^{\mu}| < 2.5$ and $\sqrt{s} = 14\,\mathrm{TeV}$. The notation of the histograms is the same as in Fig. 5. The isolation criterion as in [8–10] was applied

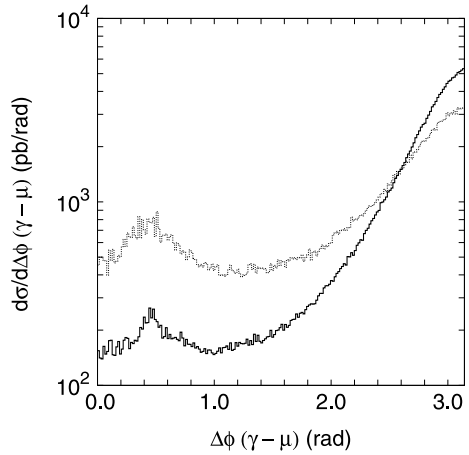

Fig. 9. The difference in azimuthal angle $\Delta\phi(\gamma - \mu)$ between the photon and muon calculated at $10\,\mathrm{GeV} < p_{\mathrm{T}} < 100\,\mathrm{GeV}$, $p_{\mathrm{T}}^{\mu} > 4\,\mathrm{GeV}$, $|\eta^{\gamma}| < 2.5$, $|\eta^{\mu}| < 2.5$ and $\sqrt{s} = 14\,\mathrm{TeV}$. The notation of the histograms is the same as in Fig. 5. The isolation criterion as in [8–10] was applied

to be perfectly compatible with the available data on the heavy quark production as well as on the production of prompt photons and various quarkonium states at modern colliders [63, 64]. It is important that the k_{T}-factorization approach succeeds in describing the polarization phenomena observed in both $p\bar{p}$ and ep interactions (see, for example, [65] and references therein). The underlying physics is essentially related to the initial gluon off-shellness, which dominates the gluon polarization properties and has a considerable impact on the kinematics. So, we believe that the k_{T}-factorization formalism holds a possible key to understanding the production dynamics at high energies. Finally, once again we would like to point out the fundamental role of angular correlations which can serve as an important and crucial test discriminating the different non-collinear evolution schemes.

4 Conclusions

We have tried a theoretical approach proposed in [29] to the associated production of prompt photons and heavy (charmed or beauty) quark in hadronic collisions at high energies. Our approach is based on the k_{T}-factorization scheme, which, unlike many early calculations [17, 20], provides solid theoretical grounds for adequately taking into account the effects of initial parton momentum. The central part of our consideration is the off-shell gluon–gluon fusion subprocess $g^* + g^* \to \gamma + q\bar{q}$. At the price of considering the $2 \to 3$ rather than $2 \to 2$ matrix elements, we have reduced the problem of unknown unintegrated quark distributions to the problem of gluon distributions. This way enables us with making comparisons between the different parton evolution schemes and parametrizations of parton densities, in contrast with previous calculations [26–28] where such a comparison was not possible (for the lack of unintegrated quark distributions except KMR).

We have calculated the total and differential $\gamma + Q$ and $\gamma + \mu$ cross sections (where muon originates from the semileptonic decay of the heavy quark Q) and have made comparisons to the recent CDF experimental data. In the numerical analysis we have used the unintegrated gluon densities obtained from the CCFM evolution equation and from the KMR prescription. It was demonstrated that the CCFM-evolved gluon density reproduces the Tevatron data very well, whereas the KMR gluon density is in disagreement with them. We especially point out the fundamental role of the angular correlations between the particles in the final state. These quantities can serve as a crucial test for the unintegrated gluon densities in a proton. Finally, we extrapolate the theoretical predictions to LHC energies.[8]

Acknowledgements. We thank H. Jung for his encouraging interest, very helpful discussions and for providing the CCFM code for unintegrated gluon distributions. The authors are very grateful to DESY Directorate for the support in the framework of Moscow – DESY project on Monte Carlo implementation for HERA – LHC. A.V.L. was supported in part by the grants of the president of Russian Federation (MK-438.2008.2) and Helmholtz – Russia Joint Research Group. Also this research was supported by the FASI of Russian Federation (Grant No. NS-8122.2006.2) and the RFBR fundation (Grant No. 08-02-00896-a).

References

1. D∅ Collaboration, B. Abbott et al., Phys. Rev. Lett. **84**, 2786 (2000)
2. D∅ Collaboration, V.M. Abazov et al., Phys. Rev. Lett. **87**, 251 805 (2001)

[8] When the present paper was prepared for publication, the D∅ collaboration presented [66] the first measurement of the prompt photon and hadronic jet associated production. The triple differential cross section $\mathrm{d}\sigma/\mathrm{d}p_{\mathrm{T}}\,\mathrm{d}\eta^{\gamma}d\eta^{\mathrm{jet}}$ has been determined in the different kinematic regions. It could also be very useful to analyze it using the off-shell $g^* + g^* \to \gamma + q\bar{q}$ matrix elements. We are planning presentation of this work in the forthcoming publications.

3. CDF Collaboration, D. Acosta et al., Phys. Rev. D **65**, 112 003 (2002)
4. CDF Collaboration, D. Acosta et al., Phys. Rev. D **70**, 032 001 (2004)
5. CDF Collaboration, D. Acosta et al., Phys. Rev. D **65**, 012 003 (2002)
6. D⊘ Collaboration, V.M. Abazov et al., Phys. Lett. B **639**, 151 (2006)
7. CDF Collaboration, F. Abe et al., hep-ex/9902001
8. CDF Collaboration, T. Affolder et al., hep-ex/0106004
9. R. Mcnulty, XXXIX Rencontres de Moriond: QCD and Hadronic Interactions, La Thuile, Italy [hep-ex/0406096]
10. A. Gajjar, XXXX Rencontres de Moriond: QCD and Hadronic Interactions, La Thuile, Italy [hep-ex/0505046]
11. K. Koller, T.F. Walsh, P.M. Zerwas, Z. Phys. C **2**, 197 (1979)
12. H.-N. Li, Phys. Lett. B **454**, 328 (1999)
13. T. Binoth, J.P. Guillet, E. Pilon, M. Werlen, Eur. Phys. J. C **16**, 311 (2000)
14. S. Catani, M. Fontannaz, J.P. Guillet, E. Pilon, JHEP **05**, 028 (2002)
15. L.E. Gordon, W. Vogelsang, Phys. Rev. D **48**, 3136 (1993)
16. H. Baer, M.H. Reno, Phys. Rev. D **54**, 2017 (1996)
17. L. Apanasevich, C. Balazs, C. Bromberg, J. Huston, A. Maul, W.K. Tung, S. Kuhlmann, J. Owens, M. Begel, T. Ferbel, G. Ginther, P. Slattery, M. Zielinski, Phys. Rev. D **59**, 074 007 (1999)
18. P. Aurenche, M. Fontannaz, J.P. Guillet, B.A. Kniehl, E. Pilon, M. Werlen, Eur. Phys. J. C **9**, 107 (1999)
19. P. Aurenche, M. Fontannaz, J.P. Guillet, B.A. Kniehl, M. Werlen, Eur. Phys. J. C **13**, 347 (2000)
20. A. Kumar, K. Ranjan, M.K. Jha, A. Bhardwaj, B.M. Sodermark, R.K. Shivpuri, Phys. Rev. D **68**, 014 017 (2003)
21. H.-L. Lai, H.-N. Li, Phys. Rev. D **58**, 114 020 (1998)
22. S. Catani, M.L. Mangano, P. Nason, C. Oleari, W. Vogelsang, JHEP **9903**, 025 (1999)
23. N. Kidonakis, J.F. Owens, Phys. Rev. D **61**, 094 004 (2000)
24. E. Laenen, G. Oderda, G. Sterman, Phys. Lett. B **438**, 173 (1998)
25. E. Laenen, G. Sterman, W. Vogelsang, Phys. Rev. Lett. **84**, 4296 (2000)
26. M.A. Kimber, A.D. Martin, M.G. Ryskin, Eur. Phys. J. C **12**, 655 (2000)
27. T. Pietrycki, A. Szczurek, Phys. Rev. D **75**, 014 023 (2007)
28. A.V. Lipatov, N.P. Zotov, J. Phys. G **34**, 219 (2007)
29. S.P. Baranov, A.V. Lipatov, N.P. Zotov, Phys. Rev. D **77**, 074 024 (2008)
30. L.V. Gribov, E.M. Levin, M.G. Ryskin, Phys. Rep. **100**, 1 (1983)
31. E.M. Levin, M.G. Ryskin, Y.M. Shabelsky, A.G. Shuvaev, Sov. J. Nucl. Phys. **53**, 657 (1991)
32. S. Catani, M. Ciafoloni, F. Hautmann, Nucl. Phys. B **366**, 135 (1991)
33. J.C. Collins, R.K. Ellis, Nucl. Phys. B **360**, 3 (1991)
34. E.A. Kuraev, L.N. Lipatov, V.S. Fadin, Sov. Phys. JETP **44**, 443 (1976)
35. E.A. Kuraev, L.N. Lipatov, V.S. Fadin, Sov. Phys. JETP **45**, 199 (1977)
36. I.I. Balitsky, L.N. Lipatov, Sov. J. Nucl. Phys. **28**, 822 (1978)
37. M. Ciafaloni, Nucl. Phys. B **296**, 49 (1988)
38. S. Catani, F. Fiorani, G. Marchesini, Phys. Lett. B **234**, 339 (1990)
39. S. Catani, F. Fiorani, G. Marchesini, Nucl. Phys. B **336**, 18 (1990)
40. G. Marchesini, Nucl. Phys. B **445**, 49 (1995)
41. V.N. Gribov, L.N. Lipatov, Yad. Fiz. **15**, 781 (1972)
42. L.N. Lipatov, Sov. J. Nucl. Phys. **20**, 94 (1975)
43. G. Altarelly, G. Parizi, Nucl. Phys. B **126**, 298 (1977)
44. Y.L. Dokshitzer, Sov. Phys. JETP **46**, 641 (1977)
45. M.A. Kimber, A.D. Martin, M.G. Ryskin, Phys. Rev. D **63**, 114 027 (2001)
46. G. Watt, A.D. Martin, M.G. Ryskin, Eur. Phys. J. C **31**, 73 (2003)
47. A.V. Bogdan, A.V. Grabovsky, Nucl. Phys. B **773**, 65 (2007)
48. CDF Collaboration, T. Affolder et al., Phys. Rev. D **65**, 052 006 (2002)
49. S.P. Baranov, N.P. Zotov, A.V. Lipatov, Yad. Fiz. **67**, 856 (2004)
50. G.P. Lepage, J. Comput. Phys. **27**, 192 (1978)
51. H. Baer, J. Ohnemus, J.F. Owens, Phys. Rev. D **42**, 61 (1990)
52. Small-x Collaboration, B. Andersson et al., Eur. Phys. J. C **25**, 77 (2002)
53. Small-x Collaboration, J. Andersen et al., Eur. Phys. J. C **35**, 77 (2004)
54. Small-x Collaboration, J. Andersen et al., Eur. Phys. J. C **48**, 53 (2006)
55. H. Jung, A.V. Kotikov, A.V. Lipatov, N.P. Zotov, in Proceedings of ICHEP'06, p. 493 [hep-ph/0 611 093]
56. H. Jung, Mod. Phys. Lett. A **19**, 1 (2004)
57. M. Glück, E. Reya, A. Vogt, Phys. Rev. D **46**, 1973 (1992)
58. M. Glück, E. Reya, A. Vogt, Z. Phys. C **67**, 433 (1995)
59. C. Peterson, D. Schlatter, I. Schmitt, P. Zerwas, Phys. Rev. D **27**, 105 (1983)
60. OPAL Collaboration, G. Abbiendi et al., Eur. Phys. J. C **8**, 573 (1999)
61. B. Bailey, E.L. Berger, L.E. Gordon, Phys. Rev. D **54**, 1896 (1996)
62. T. Sjöstrand et al., Comput. Phys. Commun. **135**, 238 (2001)
63. A.V. Lipatov, N.P. Zotov, Eur. Phys. J. C **27**, 87 (2003)
64. S.P. Baranov, Phys. Rev. D **66**, 114 003 (2002)
65. S.P. Baranov, N.P. Zotov, JETP Lett. **86**, 499 (2007)
66. D⊘ Collaboration, V.M. Abazov et al., arXiv:0804.1105 [hep-ex]